Transition-Metal Phosphinidene Complexes: Syntheses, Structures, and Bonding in Dinuclear Phosphinidene Complexes Containing 14- and 15-Electron Metal Fragments

A. M. Arif,[1a] A. H. Cowley,*[1a] N. C. Norman,[1b] A. G. Orpen,[1c] and M. Pakulski[1a]

Department of Chemistry, The University of Texas at Austin, Austin, Texas 78712, Department of Inorganic Chemistry, The University of Newcastle upon Tyne, Newcastle upon Tyne NE1 7RU, U.K., and Department of Inorganic Chemistry, The University of Bristol, Bristol BS8 1TS, U.K.

Received May 26, 1987

The reaction of $Ar'PCl_2$ ($Ar' = 2,4,6\text{-}(t\text{-}Bu)_3C_6H_2$) with $[Co(CO)_4]^-$ produces the dicobalt–phosphinidene complex $[Co_2(CO)_6(\mu\text{-}PAr')]$ (**1**), which has been characterized by X-ray crystallography. Similar reactions between $Ar'PCl_2$ and $K[Mo(CO)_3(\eta\text{-}C_5H_5)]$ and $Na_2[V(CO)_3(\eta\text{-}C_5H_5)]$ afford the phosphinidene complexes $[Mo_2(CO)_4(\eta\text{-}C_5H_5)_2(\mu\text{-}PAr')]$ (**4**) and $[V_2(CO)_4(\eta\text{-}C_5H_5)_2(\mu\text{-}PAr')]$ (**7**). Reaction of the phosphine $(TMP)PCl_2$ (TMP = 2,2,2′,2′-tetramethylpiperidino) with $K[M(CO)_3(\eta\text{-}C_5H_5)]$ (M = Mo, W) also affords the phosphinidene complexes $[M_2(CO)_4(\eta\text{-}C_5H_5)_2\{\mu\text{-}P(TMP)\}]$ [**5** (M = Mo) and **6** (M = W)]. Compounds **4**, **6**, and **7** have been characterized by X-ray crystallography. Full details of the syntheses of the above compounds are presented together with a discussion of the structures and a theoretical (EHMO) study of the bonding and electronic properties.

Introduction

Phosphinidene (or phosphanediyl, RP) ligands exhibit a versatile coordination chemistry with organo transition-metal fragments and have been observed to adopt μ_2, μ_3, and μ_4 bonding modes. Of particular interest to the present work are those which feature a μ_2-PR group. The majority of such compounds adopt the "open" structural type A, which is characterized by trigonal-planar phosphorus coordination and the absence of a metal–metal bond. Here ML_n represents a 16-electron fragment such as $M(CO)_5$ (M = Cr, Mo, W), $Mn(CO)_2(\eta\text{-}C_5H_5)$, or $Co(CO)(\eta\text{-}C_5H_5)$. These have been extensively studied by Huttner et al.[2] and more recently by Cowley[3] and Power[4] and their co-workers. Examples of type A complexes are also known for the arsenic and antimony analogues.[5] An alternative structural form or valence isomer is also possible, namely, the "closed" type B structure. While there are no examples of type B structures known for phosphorus, an antimony analogue, $[Fe_2(CO)_8\{\mu\text{-}SbCH(SiMe_3)_2\}]$, has been described[6] and a similar ditungsten complex has been postulated as an intermediate.[5m] However, examples of type B for phosphorus are known in which the phosphorus lone pair is coordinated to a third metal,[7] i.e. type C.

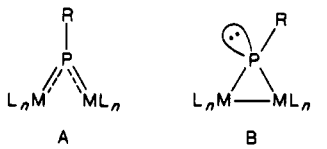

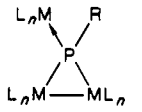

In addition to types A and B, a further group of μ_2-phosphinidene complexes exist where ML_n is a 15-electron transition-metal fragment, and it is this class of compounds that is the subject of this paper. As with complexes of types A and B, two valence isomers are possible depending on the configuration at phosphorus, namely, types D and E. The first complex of this type was described by Paine et al.[8] and featured $ML_n = Mo(CO)_2(\eta\text{-}C_5H_5)$ and R = $N(CH_3)PF_2$. However, since the crystal structure of this complex was not determined, it is unclear whether the structure adopted is of type D or E. Subsequent work by Cowley et al.[9] on complexes containing the metal fragments

(1) (a) University of Texas at Austin. (b) University of Newcastle upon Tyne. (c) University of Bristol

(2) (a) Huttner, G.; Müller, H.-D.; Frank, A.; Lorenz, H. *Angew. Chem., Int. Ed. Engl.* **1975**, *14*, 705. (b) Huttner, G.; Borm, J.; Zsolnai, L. *J. Organomet. Chem.* **1984**, *263*, C33. (c) Lang, H.; Mohr, G.; Scheidsteger, O.; Huttner, G. *Chem. Ber.* **1985**, *118*, 574. (d) Lang, H.; Orama, O.; Huttner, G. *J. Organomet. Chem.* **1985**, *291*, 293. (e) Lang, H.; Huttner, G.; Sigwarth, B.; Weber, U.; Zsolnai, L.; Jibril, I.; Orama, O. *Z. Naturforsch., B: Anorg. Chem., Org. Chem.* **1986**, *41B*, 191.

(3) Arif, A. M.; Cowley, A. H.; Norman, N. C.; Orpen, A. G.; Pakulski, M. *J. Chem. Soc., Chem. Commun.* **1985**, 1267.

(4) Flynn, K. M.; Murray, B. D.; Olmstead, M. M.; Power, P. P. *J. Am. Chem. Soc.* **1983**, *105*, 7460.

(5) RAs complexes: (a) von Seyerl, J.; Moering, U.; Wagner, A.; Frank, A.; Huttner, G. *Angew. Chem., Int. Ed. Engl.* **1978**, *17*, 844. (b) Huttner, G.; Schmid, H.-G. *Angew. Chem., Int. Ed. Engl.* **1975**, *14*, 433. (c) Huttner, G.; von Seyerl, J.; Marsili, M.; Schmid, H.-G. *Angew. Chem., Int. Ed. Engl.* **1975**, *14*, 434. (d) von Seyerl, J.; Huttner, G. *Angew. Chem., Int. Ed. Engl.* **1979**, *18*, 233. (e) Sigwarth, B.; Zsolnai, L.; Scheidsteger, O.; Huttner, G. *J. Organomet. Chem.* **1982**, *235*, 43. (f) von Seyerl, J.; Sigwarth, B.; Schmid, H.-G.; Mohr, G.; Frank, A.; Marsili, M.; Huttner, G. *Chem. Ber.* **1981**, *114*, 1392. (g) Jones, R. A.; Whittlesey, B. R. *Organometallics* **1984**, *3*, 469. (h) von Seyerl, J.; Sigwarth, B.; Huttner, G. *Chem. Ber.* **1981**, *114*, 727. (i) Hermann, W. A.; Koumbouris, B.; Zahn, T.; Ziegler, M. L. *Angew. Chem., Int. Ed. Engl.* **1984**, *23*, 812. (j) Hermann, W. A.; Koumbouris, B.; Schäfer, A.; Zahn, T.; Ziegler, M. L. *Chem. Ber.* **1985**, *118*, 2472. (k) von Seyerl, J.; Huttner, G. *Angew. Chem., Int. Ed. Engl.* **1978**, *17*, 843. (l) Weber, U.; Zsolnai, L.; Huttner, G. *J. Organomet. Chem.* **1984**, *260*, 281. (m) Weber, U.; Huttner, G.; Scheidsteger, O.; Zsolnai, L. *J. Organomet. Chem.* **1985**, *289*, 357. (n) See also: Huttner, G. *Pure Appl. Chem.* **1986**, *58*, 585 and Huttner, G.; Evertz, K. *Acc. Chem. Res.* **1986**, *19*, 406 for reviews on "inidene" complexes.

(6) (a) Cowley, A. H.; Norman, N. C.; Pakulski, M. *J. Am. Chem. Soc.* **1984**, *106*, 6844. (b) Cowley, A. H.; Norman, N. C.; Pakulski, M.; Bricker, D. L.; Russell, D. H. *J. Am. Chem. Soc.* **1985**, *107*, 8211.

(7) See for example: Schneider, J.; Huttner, G. *Chem. Ber.* **1983**, *116*, 917. Huttner, G.; Mohr, G.; Friedrich, P.; Schmid, H.-G. *J. Organomet. Chem.* **1978**, 160, 59.

(8) Light, R. W.; Paine, R. T. Maier, D. E. *Inorg. Chem.* **1979**, *18*, 2345.

(9) (a) Arif, A. M.; Cowley, A. H.; Pakulski, M. *J. Chem. Soc., Chem. Commun.* **1985**, *1707*. (b) Arif, A. M.; Cowley, A. H.; Thomas, G. J. N.; Pakulski, M. *Polyhedron* **1986**, *5*, 1651.

0276-7333/88/2307-0309$01.50/0

$M(CO)_2(\eta\text{-}C_5H_5)$ (M = Mo, W) and $Co(CO)_3$ has revealed that type D is the preferred form. Full details of the syntheses and molecular and electronic structures of these compounds are reported herein.

Results and Discussion

Synthesis and Spectroscopic Properties. Treatment of 1 equiv of $Ar'PCl_2$ (Ar' = 2,4,6-(t-Bu)$_3C_6H_2$) with 2 equiv of $K[Co(CO)_4]$ in tetrahydrofuran (THF) at room temperature affords, after chromatographic workup, the diphosphene $Ar'P{=}PAr'$;[10] and green crystalline $[Co_2(CO)_6(\mu\text{-}PAr')]$ (1). Compound 1 was shown to possess

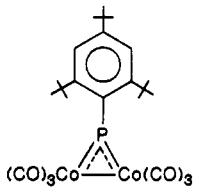

1

a type D structure by an X-ray crystallographic study, details of which will be presented in a later section. The adoption of a type D structure was also evident from the ^{31}P NMR spectrum of 1 which showed a deshielded, broad singlet at δ 664. Such deshielded signals are characteristic of type A structures involving trigonal-planar phosphorus and some degree of multiple bonding to the metal centers.[2,3,5n] Since this situation is also present in type D complexes, a deshielded ^{31}P chemical shift is also diagnostic of this structure type.

The bonding in 1 will be discussed in a later section, but it is of interest to note that the structural form with two metals (either type D or E) is probably the result of the steric demands of the Ar′ group. Thus with smaller R groups, Co_3[11,12] and Co_4[13] clusters are formed. Indeed, even

$[Co_3(CO)_9(\mu_3\text{-}PR)]$ R = Ph, t-Bu, Et_2N $[Co_4(CO)_{10}(\mu_4\text{-}PR)_2]$ R = Ph

with the relatively large $(Me_3Si)_2CH$ group only the tri- and tetranuclear cobalt complexes are formed,[14] i.e. 2 and 3, there being no evidence for a dinuclear complex analogous to 1. Such a compound may, however, be an intermediate in the formation of 2 and 3, and this may be generally true for other R groups.

$[Co_3(CO)_9\{\mu_3\text{-}PCH(SiMe_3)_2\}]$
2

$[Co_4(CO)_{10}\{\mu_4\text{-}PCH(SiMe_3)_2\}\{\mu_4\text{-}PCH_2SiMe_3\}]$
3

Another 15-electron transition-metal fragment with potential to form a complex of type D or E is $M(CO)_2(\eta\text{-}C_5H_5)$ (M = Cr, Mo, W). Accordingly the dichlorophosphine $Ar'PCl_2$ was treated with 2 equiv of $K[Mo(CO)_3(\eta\text{-}C_5H_5)]$ in THF at room temperature. Unlike the preceding cobalt reaction, a large range of phosphorus-containing products is formed. These include the known organophosphorus compounds $Ar'P{=}PAr'$,[10] $Ar'PH_2$,[10,15] $Ar'P(H)P(H)Ar'$,[10,15] and $Ar'P(H)P(Cl)Ar'$[9b] together with 4, the sole molybdenum-containing product. The adoption

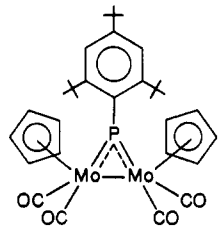

4

of a type D structure by 4 was anticipated from the low-field ^{31}P chemical shift (δ 687) and confirmed by X-ray crystallography as discussed in the next section. As mentioned in the Introduction, a similar compound, $[Mo_2(CO)_4(\eta\text{-}C_5H_5)_2(\mu\text{-}PN(Me)PF_2)]$, was reported by Paine et al.[8] The low-field ^{31}P chemical shift of this complex (δ 404.1) is consistent with a type D structure as proposed originally by the authors.[8]

A similar reaction of $(TMP)PCl_2$ (TMP = 2,2,2′,2′-tetramethylpiperidino) with 2 equiv of $K[Mo(CO)_3(\eta\text{-}C_5H_5)]$ resulted in two products, 5 and 5a, with ^{31}P NMR chemical shifts of δ 648 and 220, respectively. Crystal-

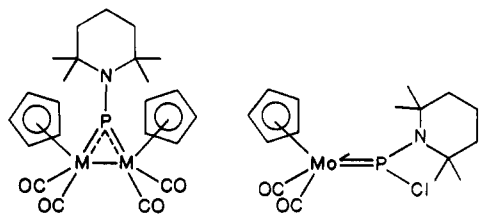

5, M = Mo
6, M = W

5a

lization from hexane at −20 °C afforded black, crystalline 5 in 30% yield. Unfortunately, crystals of 5 were unsuitable for X-ray diffraction study. The structure assignment for 5 is therefore based on analytical and spectroscopic data. If the reaction of $(TMP)PCl_2$ with $K[Mo(CO)_3(\eta\text{-}C_5H_5)]$ is carried out in a 1:1 mole ratio, the major product is 5a (D. M. Giolando, personal communication). The structure of 5a has been established by X-ray crystallography and will be reported in a future publication.

The corresponding reaction of $(TMP)PCl_2$ with $K[W(CO)_3(\eta\text{-}C_5H_5)]$ in a 1:2 mole ratio affords green, crystalline 6 as the sole tungsten-containing product. The ^{31}P chemical shift of 6 (δ 593) is very similar to that of 5 (δ 648), thus implying that both compounds possess a type D structure. In the case of 6 this was proved by X-ray crystallography (see later).

Another point of interest regarding the ^{31}P NMR data for 6 is the observation of ^{183}W satellites ($^1J_{PW}$ = 343 Hz). Typical single-bond ^{31}P–^{183}W couplings are of the order of a few hertz, the value for 6 thus providing additional evidence for P–W (or more generally P–M) multiple bonding in type D structures.

The reactions described above all give rise to dinuclear complexes containing two 15-electron transition-metal fragments. In the case of 1, 4, 5, and 6 a single phosphinidene bridge is present and the structural type adopted

(10) (a) Yoshifuji, M.; Shima, I.; Inamoto, N.; Hirotsu, K.; Higuchi, T. *J. Am. Chem. Soc.* **1981**, *103*, 4587. (b) Yoshifuji, M.; Shima, I.; Inamoto, N.; Hirotsu, K.; Higuchi, T. *J. Am. Chem. Soc.* **1982**, *104*, 6167.
(11) Markó, L.; Markó, B. *Inorg. Chim. Acta.* **1975**, *14*, L39.
(12) Beurich, H.; Madach, T.; Richter, F.; Vahrenkamp, H. *Angew. Chem., Int. Ed. Engl.* **1979**, *18*, 690.
(13) (a) Ryan, R. C.; Dahl, L. F. *J. Am. Chem. Soc.* **1975**, *97*, 6904. (b) Ryan, R. C.; Pittman, C. V.; O'Connor, J. P. *J. Organomet. Chem.* **1980**, *193*, 247.
(14) Arif, A. M.; Cowley, A. H.; Pakulski, M.; Hursthouse, M. B.; Karauloz, A *Organometallics* **1985**, *4*, 2227.
(15) (a) Cowley, A. H.; Kilduff, J. E.; Newman, T. H.; Pakulski, M. *J. Am. Chem. Soc.* **1982**, *104*, 5820. (b) Cowley, A. H.; Kilduff, J. E.; Lasch, J. G.; Mehrotra, S. K.; Norman, N. C.; Pakulski, M.; Whittlesey, B. R.; Atwood, J. L.; Hunter, W. E. *Inorg. Chem.* **1984**, *23*, 2582. (c) Cowley, A. H.; Kilduff, J. E.; Norman, N. C.; Pakulski, M. *J. Chem. Soc., Dalton Trans.* **1986**, 1801.

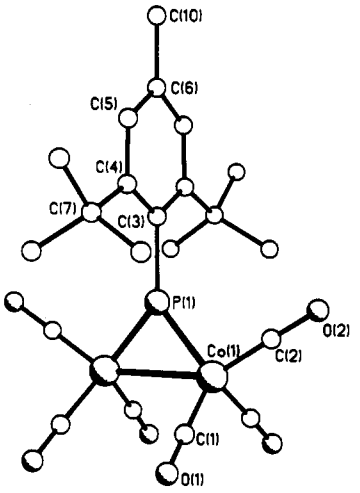

Figure 1. Molecular structure of 1 showing the atom numbering scheme adopted.

Table I. Selected Bond Distances (Å) and Angles (deg) for $[Co_2(CO)_6\{\mu\text{-}P(2,4,6\text{-}(t\text{-}Bu)_3C_6H_2)\}]$ (1)[a]

Bond Distances			
Co(1)–Co(1′)	2.690 (4)	P(1)–C(3)	1.84 (3)
Co(1)–P(1)	2.047 (6)	O(1)–C(1)	1.19 (2)
Co(1)–C(1)	1.82 (2)	O(2)–C(2)	1.22 (2)
Co(1)–C(2)	1.63 (1)		
Bond Angles			
Co(1′)–Co(1)–P(1)	49.1 (2)	Co(1)–P(1)–Co(1′)	82.0 (2)
P(1)–Co(1)–C(1)	118.9 (6)	Co(1)–P(1)–C(3)	138.9 (2)
P(1)–Co(1)–C(2)	99.6 (8)	Co(1)–C(1)–O(1)	176.7 (3)
C(1)–Co(1)–C(2)	102.5 (7)	Co(1)–C(2)–O(2)	179.2 (2)

[a] Estimated standard deviations in the least significant digit are given in parentheses in this and all subsequent tables.

is D. It was also of interest to examine a possible complex containing two 14-electron fragments. To this end the reaction of $ArPCl_2$ with $[V(CO)_3(\eta\text{-}C_5H_5)]^{2-}$ was attempted. This resulted in two vanadium-containing products, $[V(CO)_4(\eta\text{-}C_5H_5)]$ and **7**. The structure of **7** was established

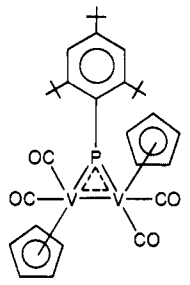

7

by X-ray crystallography. The presence of a trigonal-planar phosphorus atom is consistent with the low-field ^{31}P chemical shift (δ 657).[16]

X-ray Crystallographic Studies. The molecular structure of 1 is illustrated in Figure 1. Selected bond distances and angles are given in Table I, and atomic positional parameters are listed in Table II. Compound 1 crystallizes in the C-centered orthorhombic space group *Cmcm* and resides on two crystallographic mirror planes. The first plane coincides with the plane defined by Co(1), Co(1′), and P(1) and also includes the carbonyl C(2)–O(2) and the arene ring carbons C(3) and C(6). The second plane is orthogonal to this and contains all arene ring

Table II. Atomic Positional Parameters for $[Co_2(CO)_6\{\mu\text{-}P(2,4,6\text{-}(t\text{-}Bu)_3C_6H_2)\}]$ (1)[a]

atom	x	y	z	B,[b] Å^2
Co(1)	1.000	0.3511 (1)	0.6269 (3)	4.99 (6)
P(1)	1.000	0.2688 (4)	0.750	3.8 (2)
O(1)	1.174 (1)	0.4410 (9)	0.897 (1)	18.6 (5)
O(2)	1.000	0.273 (1)	0.403 (2)	9.3 (6)
C(1)	0.891 (2)	0.406 (1)	0.612 (2)	11.3 (6)
C(2)	1.000	0.306 (1)	0.500	6.5 (7)
C(3)	1.000	0.170 (1)	0.750	3.5 (6)
C(4)	0.909 (1)	0.1345 (9)	0.750	3.7 (4)
C(5)	0.913 (2)	0.060 (1)	0.750	5.8 (6)
C(6)	1.000	0.021 (1)	0.750	8 (1)
C(7)	0.807 (2)	0.1668 (9)	0.750	4.4 (5)
C(8)	0.790 (1)	0.209 (1)	0.869 (2)	8.7 (5)
C(9)	1.224 (2)	0.611 (1)	0.750	7.5 (8)
C(10)	1.000	−0.061 (2)	0.750	14 (1)*
C(11)	0.915 (3)	−0.098 (2)	0.750	16.3 (9)*

[a] Anisotropically refined atoms are given in the form of the isotropic equivalent thermal parameter defined as $^4/_3[a^2B(1,1) + b^2B(2,2) + c^2B(3,3) + ab(\cos\gamma)B(1,2) + ac(\cos\beta)B(1,3) + bc(\cos\alpha)B(2,3)]$ in this and subsequent tables of positional parameters. [b] Parameters with an asterisk were refined isotropically.

carbons, P(1), and the midpoint of the Co(1)–Co(1′) vector. Each cobalt atom is bonded to three terminal carbonyl ligands, of normal geometry, and the single phosphorus atom, P(1), in a tetrahedral configuration. In addition, the two cobalt atoms are mutually bonded (Co(1)–Co(1′) = 2.690 (4) Å), this separation being typical of a Co–Co single bond. The Co(1)–P(1)–Co(1′) angle (82.0 (2)°) is taken as further evidence for a metal–metal interaction. For example, in **8**, which does not contain a metal–metal bond (Co–Co = 3.89 Å), the Co–P–Co bond angle is 134.0 (2)°.[3]

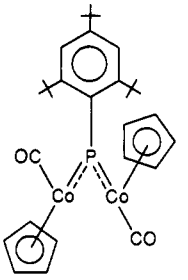

8

The Co–P distance is 2.047 (6) Å which is suggestive of significant multiple-bond character. A value of 2.05 Å has been taken to imply such bonding by Paine et al.,[17] and in **8** for which Co–P multiple bonding is also postulated,[3] values of 2.115 (4) and 2.105 (3) Å are observed. Both the Co–Co and Co–P distances are thus in accord with the bonding representation D, which will be discussed more fully in the next section. The nature of the aryl group on phosphorus also deserves some comment. The overall orientation of the arene ring plane is such that it is orthogonal to the Co_2P plane. Undoubtedly, this conformational preference is steric in origin since in this way any interaction between the ortho *t*-Bu groups and the C(2)–O(2) carbonyls is minimized. A further consequence of the conformation adopted is that the para *t*-Bu groups lie on two mirror planes. This results in complete disorder of the Me groups.

The molecular structure of **4** is shown in Figures 2 and 3, selected bond distances and angles are given in Table III, and atomic positional parameters are presented in Table IV. The structure comprises two $Mo(CO)_2(\eta\text{-}C_5H_5)$

(16) Arif, A. M.; Cowley, A. H.; Pakulski, M.; Norman, N. C.; Orpen, A. G. *Organometallics* **1987**, *6*, 189.

(17) Hutchins, L. D.; Light, R. W.; Paine, R. T. *Inorg. Chem.* **1982**, *21*, 266.

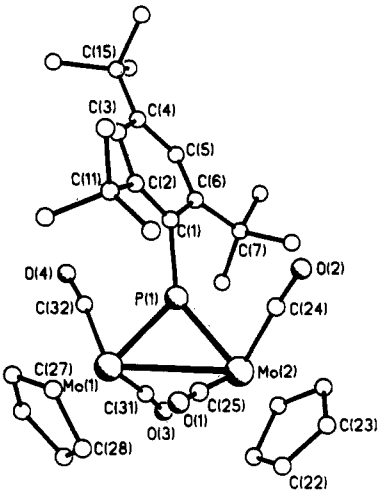

Figure 2. Molecular structure of 4 showing the atom numbering scheme adopted.

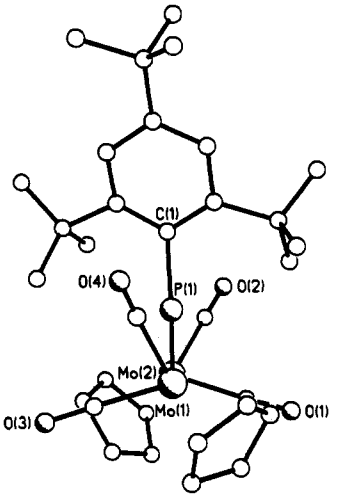

Figure 3. A view of 4 looking along the Mo(1)–Mo(2) vector showing the approximate C_2 axis.

Table III. Selected Bond Distances (Å) and Angles (deg) for $[Mo_2(CO)_4(\eta\text{-}C_5H_5)_2\{\mu\text{-}P(2,4,6\text{-}(t\text{-}Bu)_3C_6H_2)\}]$ (4)

Bond Distances			
Mo(1)–Mo(2)	3.220 (3)	Mo(1)–C(32)	2.01 (3)
Mo(1)–P(1)	2.297 (8)	Mo(2)–C(24)	1.95 (3)
Mo(2)–P(1)	2.315 (8)	Mo(2)–C(25)	1.95 (3)
P(1)–C(1)	1.89 (3)	Mo(1)–Cp(1)	2.36 (4)[a]
Mo(1)–C(31)	1.91 (3)	Mo(2)–Cp(2)	2.37 (4)[a]
Bond Angles			
P(1)–Mo(1)–Mo(2)	46.1 (3)	Mo(1)–P(1)–C(1)	127 (1)
P(1)–Mo(1)–C(31)	95.2 (9)	Mo(2)–P(1)–C(1)	144 (1)
P(1)–Mo(1)–C(32)	79.3 (9)	Mo(1)–P(1)–Mo(2)	88.4 (3)
P(1)–Mo(2)–Mo(1)	45.6 (3)	C(24)–Mo(2)–C(25)	83 (1)
P(1)–Mo(2)–C(24)	82.2 (9)	C(31)–Mo(1)–C(32)	86 (1)
P(1)–Mo(2)–C(25)	95.7 (8)		

[a] The distance quoted is an average value for all five ring carbons.

fragments linked by a Mo–Mo bond and bridged by a μ-PAr′ ligand. The geometries of the carbonyl, cyclopentadienyl, and aryl groups are normal and merit no special comment. The geometry of the Mo_2P core is the main point of interest. The Mo(1)–Mo(2) bond length of 3.220 (3) Å is typical for a Mo–Mo single bond and compares with that found in $[Mo_2(CO)_6(\eta\text{-}C_5H_5)_2]$ (3.222 Å).[18] The average Mo–P bond length is 2.306 Å. This distance

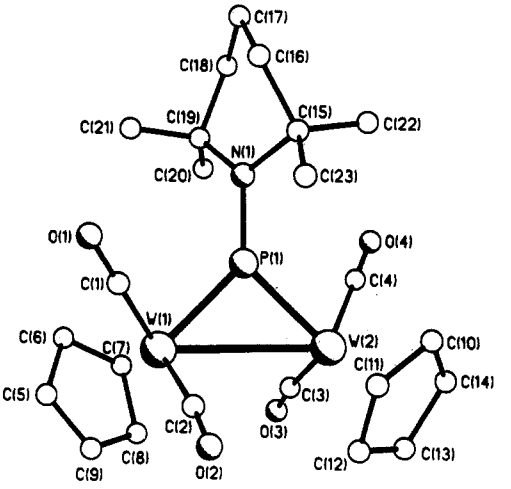

Figure 4. Molecular structure of 6 showing the atom numbering scheme adopted.

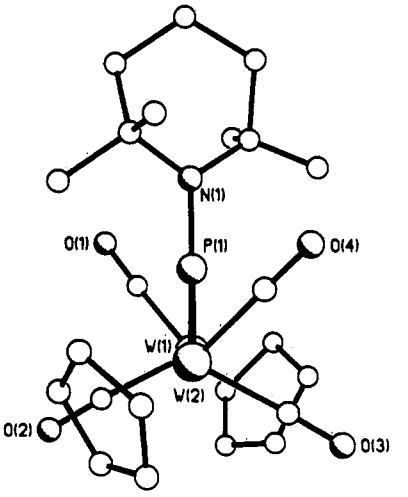

Figure 5. A view of 6 looking along the W(1)–W(2) vector showing the approximate C_2 axis.

is somewhat shorter than that for a typical Mo–P single bond (~2.35–2.40 Å), thus implying some multiple-bond character. However in 9, which contains a Mo–P bond of at least order 2, a value of 2.174 (1) Å is found.[19] In 4,

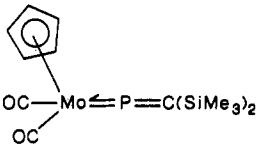

9

therefore, a Mo–P bond order between 1 and 2 is implied. We note also that, like 1, 4 exhibits an acute bridging angle at phosphorus (Mo(1)–P(1)–Mo(2) = 88.4 (3)°). As in the case of 1 the foregoing data are in accord with structure representation D.

It is evident from Figure 3 that the arene ring plane of 4 is almost perpendicular to the Mo_2P plane. As in the case of 1, this conformation presumably results from the minimization of the steric effects. It is also clear that a (noncrystallographic) twofold axis exists and is coincident with P(1) and the midpoint of the Mo(1)–Mo(2) vector. Examination of the structure of 7 will show that this feature is unlikely to be solely steric in origin but is

(18) Wilson, F. C.; Shoemaker, D. P. *J. Chem. Phys.* **1958**, *27*, 809.

(19) Cowley, A. H.; Norman, N. C.; Quashie, S. *J. Am. Chem. Soc.* **1984**, *106*, 5007.

Table IV. Atomic Positional Parameters for $[Mo_2(CO)_4(\eta\text{-}C_5H_5)_2\{\mu\text{-}P(2,4,6\text{-}(t\text{-}Bu)_3C_6H_2)\}]$ (4)[a]

atom	x	y	z	B, Å²	atom	x	y	z	B, Å²
Mo(1)	0.3758 (2)	0.3107 (2)	0.8298 (2)	2.29 (5)	C(14)	0.163 (3)	0.597 (3)	1.025 (2)	4.6 (9)
Mo(2)	0.1465 (2)	0.2589 (2)	0.7640 (1)	1.89 (4)	C(15)	0.282 (2)	0.840 (2)	0.844 (2)	2.4 (6)*
P	0.2310 (5)	0.4010 (5)	0.8049 (4)	1.8 (1)	C(16)	0.315 (3)	0.894 (3)	0.768 (2)	4.5 (9)
O(1)	0.149 (2)	0.168 (2)	0.930 (1)	4.8 (6)	C(17)	0.191 (2)	0.900 (2)	0.870 (2)	3.6 (8)
O(2)	0.037 (1)	0.632 (2)	1.185 (1)	3.5 (5)	C(18)	0.373 (2)	0.859 (2)	0.910 (2)	3.2 (7)
O(3)	0.408 (2)	0.278 (2)	0.655 (1)	6.4 (8)	C(19)	0.064 (2)	0.241 (3)	0.635 (2)	3.6 (6)*
O(4)	0.472 (2)	0.516 (2)	0.814 (2)	6.4 (8)	C(20)	0.167 (3)	0.236 (3)	0.630 (2)	4.3 (8)*
C(1)	0.218 (2)	0.537 (2)	0.815 (2)	2.8 (6)*	C(21)	0.204 (3)	0.355 (3)	1.171 (2)	4.7 (9)
C(2)	0.226 (2)	0.578 (2)	0.890 (2)	2.0 (5)*	C(22)	0.124 (2)	0.105 (2)	0.704 (2)	3.2 (6)*
C(3)	0.246 (2)	0.677 (2)	0.899 (1)	2.1 (6)	C(23)	0.039 (2)	0.159 (3)	0.681 (2)	4.0 (8)
C(4)	0.254 (2)	0.734 (2)	0.833 (2)	2.4 (6)*	C(24)	0.033 (2)	0.330 (2)	0.797 (2)	2.3 (5)*
C(5)	0.236 (2)	0.691 (2)	0.756 (2)	2.3 (6)	C(25)	0.154 (2)	0.201 (2)	0.869 (2)	2.6 (6)
C(6)	0.210 (2)	0.597 (2)	0.748 (1)	1.6 (5)*	C(26)	0.481 (2)	0.292 (3)	0.952 (2)	4.8 (9)
C(7)	0.185 (2)	0.563 (2)	0.656 (2)	2.7 (6)*	C(27)	0.386 (3)	0.242 (3)	0.956 (2)	5.0 (8)*
C(8)	0.166 (3)	0.652 (2)	0.602 (2)	5 (1)	C(28)	0.382 (3)	0.154 (3)	0.903 (2)	6 (1)
C(9)	0.078 (2)	0.507 (2)	0.652 (2)	2.3 (5)*	C(29)	0.469 (3)	0.168 (3)	0.858 (2)	5.9 (9)
C(10)	0.259 (2)	0.493 (2)	0.630 (2)	2.7 (6)*	C(30)	0.526 (3)	0.254 (3)	0.892 (2)	5.2 (9)
C(11)	0.213 (2)	0.528 (2)	0.971 (1)	1.3 (4)*	C(31)	0.391 (2)	0.291 (2)	0.721 (2)	3.4 (7)
C(12)	0.319 (2)	0.501 (3)	1.013 (2)	4.3 (8)	C(32)	0.433 (2)	0.445 (2)	0.816 (2)	3.0 (6)*
C(13)	0.143 (2)	0.439 (2)	0.962 (2)	2.7 (6)*					

[a] See footnotes *a* and *b* in Table II.

Table V. Selected Bond Distances (Å) and Angles (deg) for $[W_2(CO)_4(\eta\text{-}C_5H_5)_2(\mu\text{-}P\overline{NC(Me)_2CH_2CH_2CH_2C(Me)_2})]$ (6)

Bond Distances			
W(1)–W(2)	3.251 (1)	W(1)–C(2)	1.97 (4)
W(1)–P(1)	2.278 (7)	W(2)–C(3)	1.96 (2)
W(2)–P(1)	2.290 (7)	W(2)–C(4)	1.93 (3)
P(1)–N(1)	1.64 (2)	W(1)–Cp(1)	2.35 (4)[a]
W(1)–C(1)	1.89 (4)	W(2)–Cp(2)	2.36 (4)[a]

Bond Angles			
P(1)–W(1)–W(2)	44.8 (2)	W(1)–P(1)–N(1)	134.2 (8)
P(1)–W(1)–C(1)	81 (1)	W(2)–P(1)–N(1)	135.0 (8)
P(1)–W(1)–C(2)	99 (1)	W(1)–P(1)–W(2)	90.8 (2)
P(1)–W(2)–W(1)	44.5 (2)	C(1)–W(1)–C(2)	83 (2)
P(1)–W(2)–C(3)	100.4 (7)	C(3)–W(2)–C(4)	81 (1)
P(1)–W(2)–C(4)	81.5 (9)		

[a] See footnote *a* in Table III.

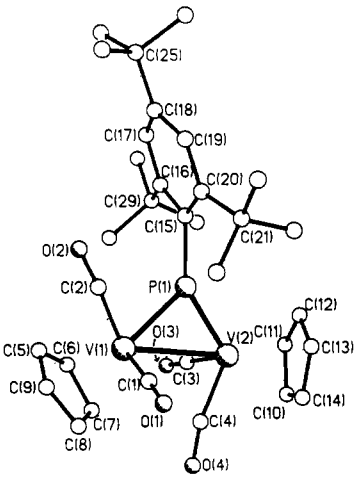

Figure 6. Molecular structure of **7** showing the atom numbering scheme adopted.

probably determined to some extent by the frontier orbital interactions in the Mo_2P ring. This aspect will be discussed in detail in the next section.

The molecular structure of **6** is shown in Figures 4 and 5, and pertinent geometric and positional parameters are assembled in Tables V and VI, respectively. Apart from the different R group (TMP instead of Ar′) the structure of **6** differs in no fundamental manner from that of **4**. The geometries and orientations of the two $W(CO_2)(\eta\text{-}C_5H_5)$ fragments in **6** are essentially identical with those of the corresponding Mo fragments in **4**. Thus an approximate C_2 axis is also present and coincident with P(1) and the W(1)–W(2) midpoint (see Figure 5). As in the case of **4** the M–M and M–P bond lengths are consistent with single and multiple bond orders, respectively, in accord with structure type D. The orientation of the TMP group is also of interest. Both the phosphorus and nitrogen atoms have a trigonal-planar coordination (sum of angles at P(1) = 360.0 (8)° and at N(1) = 360 (2)°) although it is evident

Table VI. Atomic Positional Parameters for $[W_2(CO)_4(\eta\text{-}C_5H_5)_2(\mu\text{-}P\overline{NC(Me)_2CH_2CH_2CH_2C(Me)_2})]$ (6)[a]

atom	x	y	z	B, Å²	atom	x	y	z	B, Å²
W(1)	0.4971 (1)	0.12775 (7)	0.16731 (6)	2.91 (2)	C(9)	0.338 (5)	0.023 (2)	0.223 (2)	8 (1)
W(2)	0.5101 (1)	0.32252 (7)	0.22575 (5)	2.29 (2)	C(10)	0.744 (4)	0.399 (2)	0.270 (2)	4.8 (7)
P(1)	0.5678 (8)	0.2571 (4)	0.1221 (3)	2.5 (1)	C(11)	0.761 (4)	0.313 (2)	0.290 (1)	4.2 (6)
O(1)	0.782 (3)	0.071 (2)	0.071 (1)	7.5 (7)	C(12)	0.627 (4)	0.285 (2)	0.334 (1)	5.0 (8)
O(2)	0.761 (3)	0.108 (2)	0.285 (1)	8.0 (6)	C(13)	0.531 (3)	0.355 (2)	0.345 (1)	5.5 (7)
O(3)	0.638 (2)	0.213 (2)	0.745 (1)	6.5 (6)	C(14)	0.592 (4)	0.426 (2)	0.303 (2)	6.6 (8)
O(4)	0.365 (4)	0.460 (1)	0.127 (1)	7.0 (6)	C(15)	0.799 (3)	0.344 (2)	0.042 (1)	3.5 (6)
N(1)	0.637 (3)	0.289 (1)	0.046 (1)	3.0 (4)	C(16)	0.883 (3)	0.322 (2)	−0.028 (2)	4.8 (7)
C(1)	0.673 (5)	0.093 (2)	0.110 (2)	5.8 (9)	C(17)	0.767 (4)	0.343 (2)	−0.091 (2)	5.4 (8)
C(2)	0.668 (5)	0.120 (2)	0.241 (2)	5.7 (9)	C(18)	0.583 (6)	0.337 (4)	−0.075 (2)	13 (2)
C(3)	0.274 (3)	0.295 (2)	0.235 (1)	2.8 (5)	C(19)	0.535 (3)	0.274 (2)	−0.018 (1)	4.3 (7)
C(4)	0.421 (4)	0.408 (2)	0.164 (1)	4.4 (7)	C(20)	0.366 (4)	0.290 (2)	−0.008 (2)	7.8 (6)*
C(5)	0.374 (4)	−0.006 (2)	0.160 (2)	6.9 (7)	C(21)	0.569 (8)	0.192 (3)	−0.045 (2)	17 (2)
C(6)	0.303 (4)	0.045 (2)	0.106 (2)	6.5 (8)	C(22)	0.757 (4)	0.438 (2)	0.051 (2)	5.2 (8)
C(7)	0.210 (4)	0.109 (2)	0.146 (2)	5.5 (9)	C(23)	0.915 (3)	0.307 (2)	0.099 (1)	4.3 (7)
C(8)	0.237 (5)	0.092 (2)	0.219 (2)	6.1 (8)					

[a] See footnotes *a* and *b* in Table II.

Table VII. Selected Bond Distances (Å) and Angles (deg) for $[V_2(CO)_4(\eta\text{-}C_5H_5)_2[\mu\text{-}P(2,4,6\text{-}(t\text{-}Bu)_3C_6H_2)]]$ (7)

Bond Distances			
V(1)–V(2)	2.924 (1)	V(1)–C(2)	1.883 (4)
V(1)–P(1)	2.268 (1)	V(2)–C(3)	1.925 (4)
V(2)–P(1)	2.243 (1)	V(2)–C(4)	1.917 (4)
P(1)–C(15)	1.840 (3)	V(1)–Cp(1)	2.280 (4)[a]
V(1)–C(1)	1.951 (4)	V(2)–Cp(2)	2.256 (4)[a]
Bond Angles			
P(1)–V(1)–V(2)	49.22 (3)	V(1)–P(1)–V(2)	80.83 (3)
P(1)–V(1)–C(1)	98.5 (1)	C(1)–V(1)–C(2)	90.7 (2)
P(1)–V(1)–C(2)	74.1 (1)	C(3)–V(2)–C(4)	86.7 (2)
P(1)–V(2)–V(1)	49.95 (3)	V(1)–C(1)–O(1)	177.4 (4)
P(1)–V(2)–C(3)	97.0 (1)	V(1)–C(2)–O(2)	175.8 (3)
P(1)–V(2)–C(4)	114.4 (1)	V(2)–C(3)–O(3)	177.2 (4)
V(1)–P(1)–C(15)	130.2 (1)	V(2)–C(4)–O(4)	168.0 (3)
V(2)–P(1)–C(15)	149.0 (1)		

[a] See footnote *a* in Table III.

from Figure 5 that these respective planes are almost orthogonal (124°). Thus the nitrogen lone pair, which resides in an unhybridized pure 2p orbital, can have little interaction with P(1), and the planar geometry at nitrogen is probably steric in origin. The four methyl groups also seem disposed so as to minimize any intramolecular interaction with the carbonyls C(1)–O(1) and C(4)–O(4).

Finally the structure of **7** is illustrated in Figures 6 and 7, and selected geometrical and positional parameters are listed in Tables VII and VIII, respectively. Pertinent crystallographic and data collection parameters for all four structures are summarized in Table IX in the Experimental Section. Much of the discussion presented for **4** applies also for **7**; indeed the two compounds differ effectively by only two valence electrons, both having an identical set of ligand atoms. Two major points of difference, however, warrant discussion. First the orientation of the metal fragments is different for **4** (or **6**) and **7**. This is obvious from a comparison of Figures 3 and 7, the latter of which demonstrates that for **7** a C_2 axis is no longer present. Comparison of Figures 2 and 6 reveals that this is the result of a rotation of one of the $V(CO)_2(\eta\text{-}C_5H_5)$ fragments in **7**. Since the ligand set in **4** and **7** is identical, this difference is most likely due to electronic factors, which are discussed in the next section.

The second point concerns the bond lengths in the V_2P triangle. The V–P bond lengths (average 2.255 Å) are considerably shorter than those found in vanadium–phosphine complexes (2.47–2.49 Å),[20] thus implying a

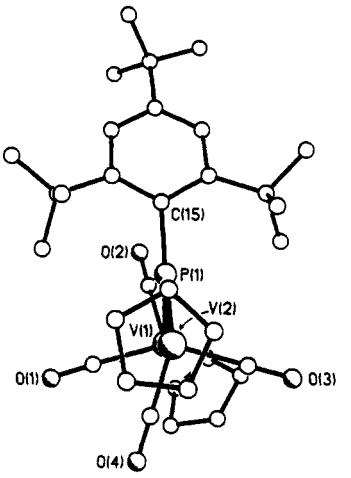

Figure 7. A view of **7** looking along the V(1)–V(2) axis.

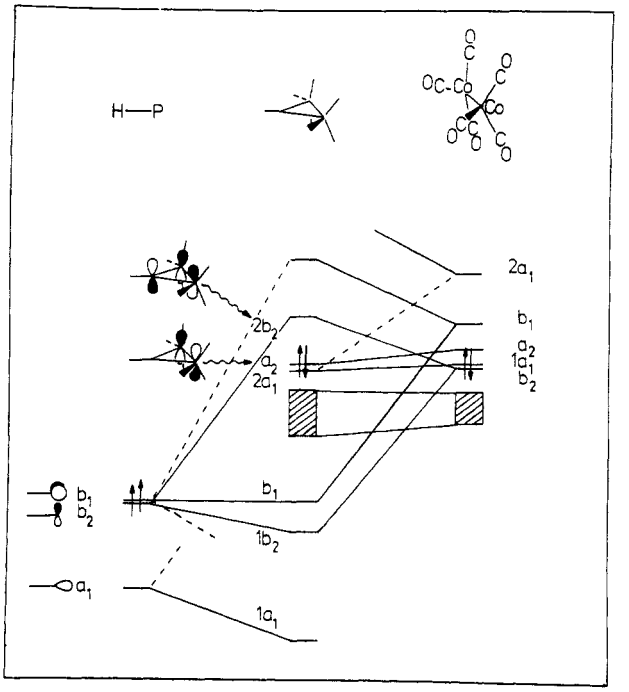

Figure 8. Important orbital interactions in **1** derived by EHMO calculations. Orbitals are labeled according to the molecular C_{2v} symmetry. The shaded block indicates a set of 6 poorly hybridized orbitals, mainly Co 3d, which play little part in Co_2P ring bonding.

Table VIII. Atomic Positional Parameters for $[V_2(CO)_4(\eta\text{-}C_5H_5)_2[\mu\text{-}P(2,4,6\text{-}(t\text{-}Bu)_3C_6H_2)]]$ (7)[a]

atom	*x*	*y*	*z*	*B*, Å²	atom	*x*	*y*	*z*	*B*, Å²
V(1)	0.3106 (1)	0.43322 (9)	0.66876 (7)	2.59 (2)	C(14)	−0.1188 (7)	0.5619 (7)	0.7556 (6)	4.4 (2)
V(2)	0.1032 (1)	0.54842 (9)	0.77735 (7)	2.61 (2)	C(15)	0.4451 (5)	0.7824 (5)	0.7756 (4)	2.0 (1)
P(1)	0.3120 (2)	0.6384 (1)	0.7541 (1)	2.23 (3)	C(16)	0.5589 (6)	0.8161 (5)	0.8529 (4)	2.4 (1)
O(1)	0.1358 (6)	0.3960 (5)	0.4712 (4)	6.0 (2)	C(17)	0.6768 (6)	0.8995 (5)	0.8489 (4)	2.8 (1)
O(2)	0.5633 (5)	0.5812 (5)	0.6181 (4)	4.9 (1)	C(18)	0.6893 (6)	0.9524 (5)	0.7775 (4)	2.4 (1)
O(3)	0.2018 (6)	0.4288 (5)	0.9219 (4)	6.6 (1)	C(19)	0.5719 (7)	0.9286 (5)	0.7101 (4)	2.9 (1)
O(4)	−0.0370 (5)	0.2833 (4)	0.6332 (4)	4.7 (1)	C(20)	0.4502 (6)	0.8475 (5)	0.7073 (4)	2.5 (1)
C(1)	0.2009 (7)	0.4125 (6)	0.5437 (5)	3.9 (2)	C(21)	0.3247 (6)	0.8396 (5)	0.6329 (4)	2.8 (1)
C(2)	0.4644 (7)	0.5285 (6)	0.6379 (5)	3.3 (2)	C(22)	0.3585 (8)	0.9261 (6)	0.5745 (5)	4.3 (2)
C(3)	0.1675 (7)	0.4719 (6)	0.8667 (5)	3.9 (2)	C(23)	0.272 (1)	0.7067 (7)	0.5577 (6)	7.2 (2)
C(4)	0.0291 (6)	0.3803 (6)	0.6839 (4)	3.2 (1)	C(24)	0.2131 (8)	0.8850 (7)	0.6938 (6)	5.3 (2)
C(5)	0.4665 (8)	0.3151 (6)	0.6684 (6)	5.2 (2)	C(25)	0.8233 (6)	1.0400 (5)	0.7720 (4)	2.9 (1)
C(6)	0.3934 (8)	0.3113 (6)	0.7450 (5)	4.6 (2)	C(26)	0.8624 (8)	0.9921 (6)	0.6676 (5)	4.3 (2)
C(7)	0.2563 (7)	0.2514 (6)	0.7044 (5)	4.0 (2)	C(27)	0.7981 (7)	1.1729 (6)	0.7935 (6)	4.7 (2)
C(8)	0.2480 (8)	0.2182 (6)	0.6018 (6)	4.4 (2)	C(28)	0.9439 (7)	1.0447 (7)	0.8461 (6)	4.8 (2)
C(9)	0.3787 (8)	0.2586 (6)	0.5795 (6)	5.2 (2)	C(29)	0.5599 (7)	0.7740 (6)	0.9431 (4)	3.1 (1)
C(10)	−0.0920 (7)	0.5425 (7)	0.8453 (6)	4.7 (2)	C(30)	0.6837 (9)	0.8499 (8)	1.0246 (5)	5.9 (2)
C(11)	0.0073 (8)	0.6465 (7)	0.9106 (5)	4.6 (2)	C(31)	0.5714 (8)	0.6348 (6)	0.9142 (5)	4.2 (2)
C(12)	0.0407 (7)	0.7300 (6)	0.8619 (5)	4.0 (2)	C(32)	0.4315 (8)	0.7921 (7)	0.9940 (5)	4.4 (2)
C(13)	−0.0370 (7)	0.6797 (6)	0.7677 (5)	4.2 (2)					

[a] See footnote *a* in Table II.

Table IX. Crystallographic and Intensity Data Collection Parameters for 1, 4, 6, and 7

	1	4	6	7
formula	$C_{24}H_{29}Co_2PO_6$	$C_{32}H_{39}Mo_2PO_4$	$C_{23}H_{28}W_2PNO_4$	$C_{32}H_{39}V_2PO_4$
fw	562.33	710.59	781.16	620.52
crystal class	orthorhombic	monoclinic	monoclinic	triclinic
space group	*Cmcm* (No. 63)	$P2_1/c$ (No. 14)	$P2_1/n$	$P\bar{1}$ (No. 2)
a, Å	13.767 (3)	13.429 (2)	8.065 (4)	9.954 (2)
b, Å	18.735 (2)	13.705 (2)	15.661 (3)	11.562 (2)
c, Å	10.933 (3)	17.072 (2)	19.225 (5)	14.362 (3)
α, deg				109.82 (2)
β, deg		97.62 (1)	90.27 (4)	94.09 (2)
γ, deg				100.85 (2)
U, Å^3	2820.2 (5)	3114 (1)	2428 (3)	1511 (1)
Z	4	4	4	2
ρ(calcd), g cm^{-3}	1.324	1.515	2.136	1.364
radiatn	graphite monochromated Mo radiation, λ = 0.710 69 Å			
μ(Mo Kα), cm^{-1}	12.6	8.7	97.6	6.8
% decay of std	13.5	3.7	3.2	2.9
2θ range, deg	$2.0 \leq 2\theta \leq 50.0$	$2.0 \leq 2\theta \leq 50.0$	$3.0 \leq 2\theta \leq 48.0$	$3.0 \leq 2\theta \leq 48.0$
reflecns measd	1416	5925	4077	5043
reflecns obsd	1372	3007	3785	4732
data omission factor	$I > 3.0\sigma(I)$			
R^a	0.0907	0.0870	0.0601	0.0498
$R_w{}^b$	0.1088	0.0910	0.0718	0.0562
no. of variables	126	277	275	512
GOF^c	6.377	5.498	5.435	3.920
p^d		0.04	0.03	0.07

$^a R = \sum(|F_o| - |F_c|)/\sum|F_o|^2$. $^b R_w = [\sum_w(|F_o| - |F_c|)^2/\sum|F_o|^2]^{1/2}$. ^{c}GOF = $[\sum_w(|F_o| - |F_c|)^2/(NO - NV)]^{1/2}$. ^{d}The weighting scheme used was of the form $w = 4F_o^2/\sigma^2(F_o)^2$ and $\sigma^2(F_o)^2 = \sigma_o^2(F_o)^2 + (pF^2)^2$. *p* is an empirical factor used to downweight intense reflections. NO = number of observed data. NV = number of parameters varied.

modicum of multiple bonding. The nature of the V–V bond is more ambiguous, however. With two 15-electron fragments present (e.g., **4**), only a M–M single bond is required as represented in structure D. In contrast, a formal double bond is required for two 14-electron fragments attached to a trigonal-planar phosphorus atom (representation F) if an 18-electron count is to be achieved at each metal. The assignment of metal–metal bond order

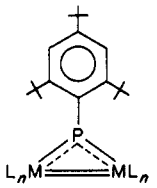

F

on the basis of their mutual bond distance tends to be ambiguous when bridging ligands are present.[21] However, the available data suggest that a V–V distance of 2.200 (2) Å (In $V_2(2,6\text{-}(MeO)_2Ph)_4\cdot THF$)[22] corresponds to a triple bond, while lesser degrees of V–V multiple bonding have been suggested for the compounds $[V_2(CO)_5(\eta\text{-}C_5H_5)_2]$ (2.462 (2) Å),[20b,23] $[V_2(CO)_5(PPh_3)(\eta\text{-}C_5H_5)_2]$ (2.466 (1) Å),[20b] $[V_2(H)_2(\eta\text{-}C_5H_5)_2(\mu\text{-}C_6H_6)]$ (2.425 (1) Å),[24] and $[V_2(CO)_8(\mu\text{-}PMe_2)_2]$ (2.733 Å).[25] Clearly the V–V distance in **7** (V(1)–V(2) = 2.924 (1) Å) is not indicative of substantial multiple-bonding character. Nevertheless, as in the structures of **1**, **4**, and **6**, a metal–metal interaction is strongly implied by the acute angle at phosphorus (V(1)–P(1)–V(2) = 80.83 (3)°).

A final noteworthy feature of the structure of **7** is that one carbonyl, C(4)–O(4), has a slightly smaller angle at carbon (V(2)–C(4)–O(4) = 168.0 (3)°) than the other three (average angle at carbon = 176.8 (4)°). It may thus be described as almost semibridging (see Figure 6), a view consistent with the low CO stretching frequency of 1855 cm^{-1} (see Experimental Section).

Theoretical Studies

The electronic structures of **1** and **7** have been characterized by molecular orbital calculations on the model compounds $[Co_2(CO)_6(\mu\text{-}PH)]$ and $[V_2(CO)_4(\eta\text{-}C_5H_5)_2(\mu\text{-}PH)]$, respectively. The geometries were derived from the crystal structures of **1** and **7**, with C–H bond distances set to 1.09 Å, P–H to 1.44 Å, and C_5H_5 rings constrained to D_{5h} symmetry with C–C = 1.42 Å. All calculations were carried out by the extended Hückel method,[26] with orbital exponents and H_{ij}'s taken from the literature.[26-28] Figure 8 illustrates the important interactions in the Co_2P ring system of **1**. The frontier orbitals of the $Co_2(CO)_6$ fragment in a sawhorse geometry, as here, have been discussed in detail by Hoffmann and Thorn.[28]

The electronic structures of **1** and **7** (and hence **4** and **6**) are best approached by consideration of the fragments from which they may be constructed. The frontier orbitals of the conical C_{3v}-d^9-ML_3 fragment (e.g. $Co(CO)_3$) and C_s-d^4-$CpML_2$ fragment (e.g. $V(CO)_2(\eta\text{-}C_5H_5)$) have been elaborated by Hoffmann et al.[29,30] These authors have

(20) (a) Schneider, M.; Weiss, E. *J. Organomet. Chem.* **1976**, *121*, 189. (b) Huffmann, J. C.; Lewis, L. N.; Caulton, K. G. *Inorg. Chem.* **1980**, *19*, 2755.
(21) Cotton, F. A.; Walton, R. A. In *Multiple Bonds Between Metal Atoms*; Wiley: New York, 1982.
(22) Cotton, F. A.; Millar, M. *J. Am. Chem. Soc.* **1977**, *99*, 7886.
(23) (a) Cotton, F. A.; Frenz, B. A.; Kruczynski, L. *J. Am. Chem. Soc.* **1973**, *95*, 951. (b) Cotton, F. A.; Kruczynski, L.; Frenz, B. A. *J. Organomet. Chem.* **1978**, *160*, 93.
(24) Jonas, K.; Wiskamp, V.; Tsay, Y.-H.; Krüger, C. *J. Am. Chem. Soc.* **1983**, *105*, 5480.
(25) Vahrenkamp, H. *Chem. Ber.* **1978**, *111*, 3472. For a theoretical discussion of this molecule see: Shaik, S.; Hoffman, R. *J. Am. Chem. Soc.* **1980**, *102*, 1194.
(26) Howell, J.; Rossi, A.; Wallace, D.; Harak, I. K.; Hoffmann, R. *QCPE* **1977**, *10*, 344.
(27) Kubacek, P.; Hoffmann, R.; Harlaz, Z. *Organometallics* **1982**, *1*, 180.
(28) Thorn, D. L.; Hoffmann, R. *Inorg. Chem.* **1978**, *17*, 126.
(29) Elian, M.; Hoffmann, R. *Inorg. Chem.* **1975**, *14*, 1058.
(30) Schilling, B. E. R.; Hoffmann, R.; Lichtenberger, D. L. *J. Am. Chem. Soc.* **1979**, *101*, 585.

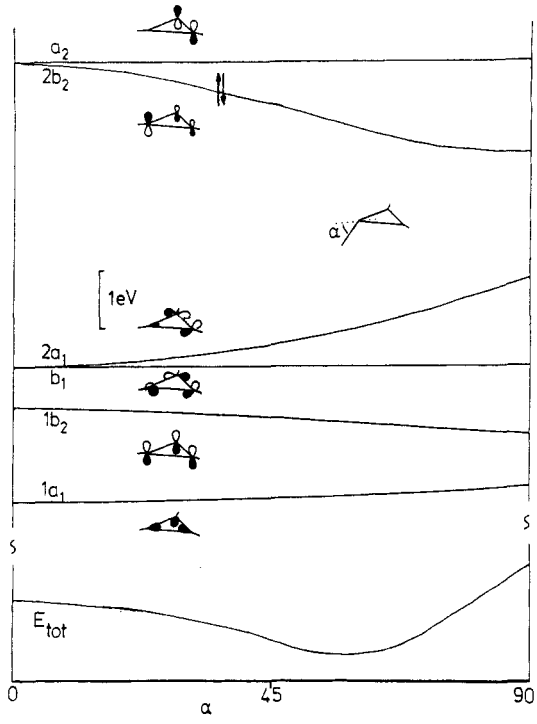

Figure 9. Walsh diagram for out-of-plane deformation of α degrees at one carbon atom of $C_3H_3^-$. Total energy is plotted below, indicating an equilibrium structure with $\alpha \approx 60°$.

shown that these fragments are isolobal[31] with CH and CH^+, respectively, and therefore that d^5-$CpML_2$ (as $M(CO)_2(\eta\text{-}C_5H_5)$ (M = Mo, W)) is isolobal with CH. Thus each of these metal–ligand units has one σ and two, orthogonal, π frontier orbitals. Finally, the PR (R = Ar', TMP) fragment present in each of the complexes is clearly isolobal with CR^-. Therefore, to a first approximation, complexes **1**, **4**, **6**, and **7** are isolobal with $C_3R_3^-$, $C_3R_3^-$, $C_3R_3^-$, and $C_3R_3^+$, respectively. The isolobal analogy is clearly inadequate here since the D_{3h}-$C_3R_3^-$ (cyclopropenide) anion (the analogue of structure type D) is Jahn–Teller unstable with respect to a C_s isomer (the analogue of structure type E). However, the actual calculations indicate that there is merit in the broad outline provided by the isolobal analogy. As shown in Figure 8, the in-plane and out-of-plane orbitals match those expected for a planar c-C_3R_3 unit (Figure 9), at least in terms of nodal characteristics. The in-plane orbitals (labeled $1a_1$, b_1, and $2a_1$, for planar $C_3H_3^-$ in Figure 9 to emphasize the relationship with C_{2v}-$[Co_2(CO)_6(\mu\text{-}PR)]$ in Figure 8) are combinations of fragment σ and π orbitals within the three-atom plane.

The ring π system is developed from the out-of-plane fragment π orbitals. There is a low-lying symmetric combination ($1b_2$ in C_{2v}) and a pair of high-lying orbitals, each with one nodal plane normal to the ring. These transform as a_2 and $2b_2$ in C_{2v} symmetry but are degenerate in D_{3h}, the highest symmetry of planar C_3H_3. in $C_3H_3^+$, the cyclopropenium cation, this high-lying pair of orbitals is unoccupied and a planar D_{3h} equilibrium structure results. In $C_3H_3^-$, the cyclopropenide anion, the degenerate orbitals are occupied by two electrons and a first-order Jahn–Teller effect results. As illustrated in Figure 9, the degeneracy of this upper π set is lost on lowering the molecular symmetry (to C_s) by a deformation toward a type E structure. The stabilization that results from pyramidalization at one carbon atom is due primarily to the fall in energy of the HOMO (labeled $2b_2$ in Figure 9).

In contrast, the organometallic complexes **1** and **7** show an orbital pattern in which $2b_2$ is *above* a_2 (see ref 16 for the interaction diagram for **7**). In **1**, a_2 and $2b_2$ are the HOMO and the LUMO, respectively, and there is a significant HOMO–LUMO energy gap (0.85 eV). The nodal characteristics of these orbitals in **1** (and **7**) are the same as those for the similarly labeled orbitals of $C_3H_3^-$ shown in Figure 9. However, important differences exist betwen **1** (and **4** and **6**) and their organic analogue $C_3H_3^-$. Because of the lower symmetry (C_{2v} at most) no first-order Jahn–Teller effect can operate, driving a distortion of the D → E type. In fact (as for $C_3H_3^-$) such a distortion, which causes pyramidalization at phosphorus in **1**, lowers the energy of "$2b_2$" but leaves a_2 unchanged. Since $2b_2$ is the LUMO of **1**, no stabilization results, and in the limit of full pyramidalization at phosphorus, a crossing (of a_2 by $2b_2$) occurs and the D → E distortion is forbidden. The crucial difference between the electronic structures of **1** and $C_3H_3^-$ lies in the greater destabilization that results from P···Co π-antibonding (as in $2b_2$) as compared with the Co···Co π-antibonding interactions (as seen in a_2). Thus poor Co···Co π overlap causes a_2 to lie below $2b_2$. For **7**, whereas a_2 is the LUMO, there is also no tendency for out-of-plane distortion at phosphorus, just as is the case for its organic analogue $C_3H_3^+$.

As discussed above, on the basis of the effective atomic number rule, the *formal* V–V bond order in **7** is 2, but the V–V distance is rather long. The analogy between **7** and the cyclopropenium cation also leads to a V–V bond order greater than 1, but where the amount of multiple bonding depends critically on the vanadium contribution to $1b_2$, the site of V–V π bonding. In fact, due to the greater electronegativity of the phosphorus 3p π orbital component, the $1b_2$ orbital is largely localized on phosphorus, and little V–V multiple bonding is calculated to result. The metal–metal distances in **1**, **4**, and **6** are at the long end of the range known for homometallic single bonds for Co, Mo, and W, respectively. This is consistent with the orbital analysis given here. Occupany of a_2, the HOMO in these molecules, leads to reduction of the formal metal–metal bond order to 1, and to a longer equilibrium metal–metal distance.

As noted in the discussion of the structures of **4**, **6**, and **7**, the $M(CO_2)(\eta\text{-}C_5H_5)$ units vary in conformation relative to the M_2P plane. As a measure of this variation the angles between the line joining two carbonyl carbons bound to a metal atom and the M_2P plane were calculated. These values are 21.8 and 23.1° for **4**, 14.5 and 10.7° for **6**, and 35.2 and 64.2° for **7**. Hoffmann et al.[30] have pointed out that the two π frontier orbitals of the $CpML_2$ fragment are not equivalent in degree of hybridization or energy. These authors showed that the π orbital with its nodal plane bisecting the two CO ligands (i.e. with its lobes in a plane *parallel* to the line joining the two carbonyl carbons) is better hybridized for π bonding than the other orthogonal, slightly lower energy π orbital. This leads to weak orientational preferences in $CpML_2$(ligand) complexes.[30] It is notable that in **7** the $V(CO)_2(\eta\text{-}C_5H_5)$ orientations allow the fragment π function contributing to the $1b_2$ orbital (i.e. the V–P bonding) to be largely composed of the better hybridized π orbital. In particular V(2) is rather close to the optimum orientation for V–P π bonding (C···C inclined at 64.2° to V_2P plane, cf. 35.2° for V(1)) and shows the shorter V–P distance. The orientations observed in the Mo_2 and W_2 species allow the poorly hybridized π functions to form the a_2 M–M π^* orbital, presumably causing it to be less severly destabilized.

(31) Hoffmann, R. *Angew. Chem., Int. Ed. Engl.* **1982**, *27*, 711.

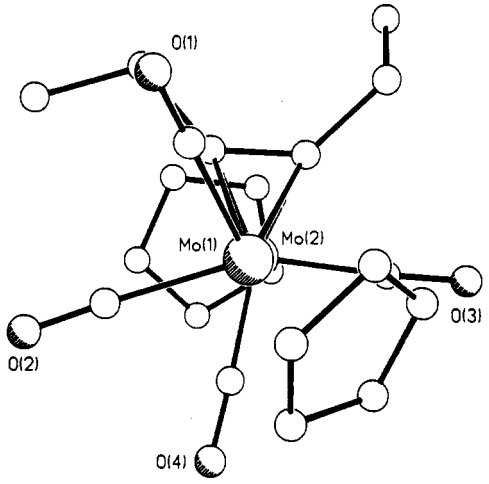

Figure 10. A view of $[Mo_2(CO)_4(\eta\text{-}C_5H_5)_2(\mu\text{-}EtC{\equiv}CEt)]$ looking along the Mo–Mo vector. The figure was drawn from coordinates taken from ref 32a.

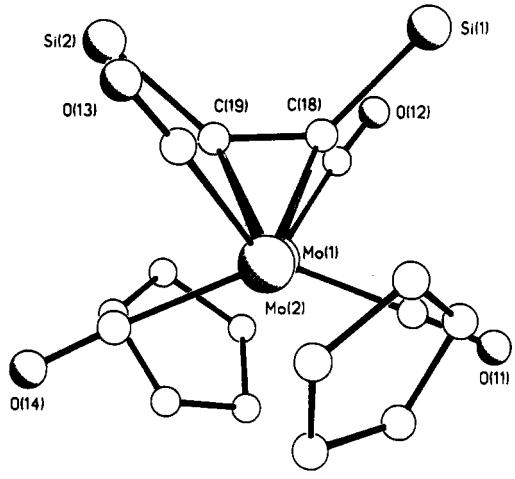

Figure 11. A view of $[Mo_2(CO)_4(\eta\text{-}C_5H_5)_2(\mu\text{-}Me_3SiC{\equiv}CSiMe_3)]$ looking along the Mo–Mo vector. Methyl groups on the Me_3Si groups are omitted for clarity. The figure was drawn from coordinates taken from ref 32b.

We note that in C_{2v} symmetry the four-electron PH fragment has frontier orbitals of a_1, b_1, and b_2 symmetry and thus binds successfully to $M_2(CO)_4(\eta\text{-}C_5H_5)_2$ and $Co_2(CO)_6$ moieties. A similar situation obtains for the binding of cis-bent acetylenes to these dimetal units. The electronic structures of these acetylene complexes and related species have been studied by a number of groups (e.g. ref 28 and references therein and ref 32). With particular regard to acetylene complexes of the $M_2(CO)_4(\eta\text{-}C_5H_5)_2$ fragment it is interesting to note that similar conformations are observed. Views of $[Mo_2(CO)_4(\eta\text{-}C_5H_5)_2(\mu\text{-}EtC{\equiv}CEt)]$[32a] and $[Mo_2(CO)_4(\eta\text{-}C_5H_5)_2(\mu\text{-}Me_3SiC{\equiv}CSiMe_3)]$[32b] are shown in Figures 10 and 11, respectively. It is apparent that the conformation of the former alkyne complex is similar to that found in **7**, while that in the latter is similar to **4** and **6**. It has already been stated that the electronic factors that influence these conformations are relatively small. This is an important point since the steric constraints placed on the geometries of **1**, **4**, **6**, and **7** by the large substituents at phosphorus and similar constraints in the alkyne complexes cannot be ignored. These may well play a role in determining the equilibrium geometries of these complexes.

We note also that the low-lying empty $2b_2$ orbital, substantially centered on phosphorus, is presumably the cause of the low-field ^{31}P chemical shifts observed for **1** and **7** and, by inference for **4**, **5**, and **6**. As discussed by Fenske et al.[33] for carbyne and carbene complexes, such low-lying unoccupied orbitals cause large paramagnetic contributions to chemical shifts and are the likely site of nucleophilic attack (steric factors permitting). Huttner[5n,34] has indicated that a similar LUMO, centered on P, is present in μ-phosphinidene complexes without metal–metal bonds.

Experimental Section

General Procedures. All experiments were performed under an atmosphere of dry dinitrogen by using standard Schlenk techniques. All solvents were freshly distilled over CaH_2 or Na/benzophenone immediately prior to use.

Spectroscopic Measurements. ^1H and ^{13}C NMR spectra were recorded on a Nicolet NT200 or Bruker WH300 spectrometer operating at 200 or 300.13 MHz, respectively, for ^1H and 50 or 75.47 MHz, respectively for ^{13}C. ^{31}P NMR spectra were recorded on Varian FT80A, Nicolet NT200, and Bruker WH300 spectrometers operating at 32.38, 80.99, and 121.49 MHz, respectively. ^1H and ^{13}C spectra were referenced to Me_4Si (δ 0.0) and ^{31}P spectra to 85% H_3PO_4 (δ 0.0), positive values to high frequency in all cases.

Medium- and high-resolution mass spectra (HRMS) were measured on Du Pont Consolidated Model 21-491 and 21-2100 instruments, respectively, the latter calibrated by using perfluorokerosene.

Infrared spectra were recorded in hexane solution on a Perkin-Elmer 1330 spectrophotometer.

Starting Materials. The organometallic anions $K[Co(CO)_4]$[35] and $Na_2[V(CO)_3(\eta\text{-}C_5H_5)]$[36] and the halophosphines 2,4,6-$(t\text{-}Bu)_3C_6H_2PCl_2$,[37] $(TMP)PCl_2$,[38] and $(Me_3Si)_2CHPCl_2$[39] were prepared by literature methods. $K[M(CO)_3(\eta\text{-}C_5H_5)]$ (M = Mo, W) was prepared by potassium amalgam reduction of the corresponding dimer. All other materials were procured commercially and used as supplied.

Preparation of $[Co_2(CO)_6\{\mu\text{-}P(2,4,6\text{-}(t\text{-}Bu)_3C_6H_2)\}]$ (1). A solution of $Ar'PCl_2$ (1.737 g, 5 mmol) in THF (25 mL) was prepared, cooled to −78 °C, and stirred. To this was added slowly a solution of $K[Co(CO)_4]$ (10 mmol) in THF (110 mL), causing a color change to green. The reaction mixture was then allowed to warm to room temperature and stir overnight. The THF was removed in vacuo and the crude reaction mixture redissolved in hexane. Purification was effected by column chromatography (silica gel; hexane), yielding Ar'P=PAr' (0.14 g, 10%) and **1** (1.6 g, 57%). Crystals of **1** were obtained from hexane at −20 °C. Physical data for **1**: mp 322–325 °C; IR ν_{C-O} (hexane) 2020 (s), 2070 (s) cm^{-1}; ^1H NMR (C_6D_6) δ 1.45 (s, 9 H, para *t*-Bu), 1.55 (s, 18 H, ortho *t*-Bu), 7.45 (s, br, 2 H, C_6H_2); $^{31}P\{^1H\}$ NMR (CH_2Cl_2) δ 664. Anal. Calcd for $C_{24}H_{29}Co_2O_6P$: C, 51.26; H, 5.20. Found: C, 51.61; H, 5.24.

Preparation of $[Mo_2(CO)_4(\eta\text{-}C_5H_5)_2\{\mu\text{-}P(2,4,6\text{-}(t\text{-}Bu)_3C_6H_2)\}]$ (4). A solution of $Ar'PCl_2$ (1.737 g, 5 mmol) in THF (25 mL) was prepared and stirred at room temperature. To this was added slowly a solution of $K[Mo(CO)_3(\eta\text{-}C_5H_5)]$ (10 mmol), causing a color change to dark brown. ^{31}P NMR assay indicated the presence of **4**, Ar'P=PAr', $Ar'PH_2$, Ar'P(H)P(Cl)Ar', and Ar'P(H)P(H)Ar', the details of which are discussed in ref 9b. Compound **4** was obtained in a pure state by column chromatography

(32) (a) Bailey, W. I.; Chisholm, M. H.; Cotton, F. A.; Rankel, L. A. *J. Am. Chem. Soc.* **1978**, *100*, 5764. (b) Beck, J. A.; Knox, S. A. R.; Stanfield, R. F. D.; Stone, F. G. A.; Winter, M. J. *J. Chem. Soc., Dalton Trans.* **1982**, 195.

(33) Fenske, R. F. *Organometallic Compounds*; Shapiro, B. L., Ed.; TX, 1983; p 305.

(34) Huttner, G. *J. Organomet. Chem.* **1986**, *308*, C11.

(35) Edgell, W. F.; Lyford, J. *Inorg. Chem.* **1970**, *9*, 1932.

(36) Fischer, E. O.; Schneider, R. J. *Chem. Ber.* **1970**, *103*, 3684.

(37) Yoshifuji, M.; Shima, I.; Inamoto, N.; Hirotsu, K.; Higuchi, T. *J. Am. Chem. Soc.* **1981**, *103*, 4587.

(38) King, R. B.; Sadanani, N. D. *Synth. React. Inorg. Met.-Org. Chem.* **1985**, *15*, 149.

(39) (a) Gynane, M. J. S.; Hudson, A.; Lappert, M. F.; Power, P. P. *J. Chem. Soc., Chem. Commun.* **1976**, 623. (b) Gynane, M. J. S.; Hudson, A.; Lappert, M. F.; Power, P. P. Goldwhite, H. *J. Chem. Soc., Dalton Trans.* **1980**, 2428.

of the crude reaction mixture (silica gel; hexane/toluene, 5:1) after removal of the THF in vacuo. Yellow-brown crystals of **4** (0.6 g, 17%) were obtained from hexane at −20 °C. Physical data for **4**: IR $\nu_{C=O}$ (hexane) 1955 (s), 1920 (s), 1880 (s), 1860 (s) cm^{-1}; ^1H NMR (C_6D_6) δ 1.34 (s, 9 H, para-*t*-Bu), 1.50 (s, 18 H, ortho *t*-Bu), 5.15 (s, 10 H, C_5H_5), 7.60 (d, 2 H, C_6H_2, $^4J_{PH}$ = 2.5 Hz); $^{31}P\{^1H\}$ NMR (CH_2Cl_2) δ 687. Anal. Calcd for $C_{32}H_{39}Mo_2O_4P$: C, 54.10; H, 5.53. Found: C, 54.69; H, 5.68.

Preparation of $[Mo_2(CO)_4(\eta\text{-}C_5H_5)_2\{\mu\text{-}PNC(Me)_2CH_2CH_2CH_2C(Me)_2\}]$ (5). A solution of $(TMP)PCl_2$ (1.21 g, 5 mmol) in THF (25 mL) was prepared and stirred at room temperature. A solution of $K[Mo(CO)_3(\eta\text{-}C_5H_5)]$ (10 mmol) was slowly added, slowly causing a darkening of color. Removal of the THF in vacuo, dissolution of the crude product in hexane, and purification by column chromatography (silica gel; hexane/toluene, 2:1) yielded a black fraction showing two ^{31}P NMR signals at δ 648 (**5**) and 220 (**5a**). Crystallization from hexane at −20 °C gave black crystals (0.9 g, 30%) of **5** although these were unsuitable for X-ray diffraction. Physical data: IR $\nu_{C=O}$ (hexane) 2020 (m, br), 1960 (m, br) cm^{-1}; ^1H NMR (C_6D_6) δ 1.25 (m, 6 H, CH_2), 1.46 (s, 12 H, CH_3), 5.15 (s, 10 H, C_5H_5). Anal. Calcd for $C_{23}H_{28}Mo_2NO_4P$: C, 45.64; H, 4.66. Found: C, 45.21; H, 4.85.

Preparation of $[W_2(CO)_4(\eta\text{-}C_5H_5)_2\{\mu\text{-}PNC(Me)_2CH_2CH_2CH_2C(Me)_2\}]$ (6). This compound was prepared and purified in an exactly analogous manner to that of **5** but using $K[W(CO)_3(\eta\text{-}C_5H_5)]$. Green crystals were obtained from hexane at −20 °C (1.7 g, 44%). Physical data for **6**: mp 151–155 °C (decomp); IR $\nu_{C=O}$ (hexane) 1890 (s, br), 1850 (m, br) cm^{-1}; ^1H NMR (C_6D_6) δ 1.23 (m, 6 H, CH_2), 1.44 (s, 12 H, CH_3), 5.13 (s, 10 H, C_5H_5); $^{31}P\{^1H\}$ NMR (CH_2Cl_2) δ 593 ($^1J_{PW}$ = 343 Hz). Anal. Calcd for $C_{23}H_{28}W_2NO_4P$: C, 35.37; H, 3.61. Found: C, 35.62; H, 3.69.

Preparation of $[V_2(CO)_4(\eta\text{-}C_5H_5)_2\{\mu\text{-}P(2,4,6\text{-}(t\text{-}Bu)_3C_6H_2)\}]$ (7). A solution of $Ar'PCl_2$ (1.734 g, 5 mmol) in THF (25 mL) was treated with a suspension of $Na_2[V(CO)_3(\eta\text{-}C_5H_5)]$ (5 mmol) in THF (100 mL), and the resulting mixture was stirred at room temperature for 2 h. After removal of the THF in vacuo the dark residue was extracted with hexane giving a yellow-green solution. Purification by column chromatography (Florisil) gave a yellow solution of $[V(CO)_4(\eta\text{-}C_5H_5)]$ on elution with hexane followed by a dark green solution of **7** on elution with hexane/5% Et_2O. Crystals of **7** (0.93 g, 30%) were obtained from hexane at −20 °C. Physical data for **7**: IR $\nu_{C=O}$ (hexane) 1985 (m), 1930 (s), 1910 (s), 1855 (m) cm^{-1}; ^1H NMR (C_6D_6) δ 1.48 (s, 18 H, ortho *t*-Bu), 1.62 (s, 9 H, para *t*-Bu), 5.36 (s, 10 H, C_5H_5), 8.08 (d, 2 H, C_6H_2, $^4J_{PH}$ = 2.5 Hz); $^{13}C\{^1H\}$ NMR (C_6D_6) δ 153.4 and 152.0 (aromatic ring carbons), 124.3 (d, $^3J_{PC}$ = 8 Hz, meta-C_6H_2), 99.5 (C_5H_5), 39.6 and 35.5 (quaternary *t*-Bu carbons), 34.1 (ortho *t*-Bu), 32.1 (para *t*-Bu); $^{31}P\{^1H\}$ NMR (C_6D_6) δ 657. Anal. Calcd for $C_{32}H_{39}V_2PO_4$: C, 61.94; H, 6.34. Found: C, 61.57; H, 6.23.

X-ray Analysis of $[Co_2(CO)_6\{\mu\text{-}P(2,4,6\text{-}(t\text{-}Bu)_3C_6H_2)\}]$ (1). A suitable single crystal of **1** was sealed in a Lindemann capillary and mounted on an Enraf-Nonius CAD4-F diffractometer. Initial lattice parameters were determined from a least-squares fit to 25 accurately centered reflections, $15 \leq 2\theta \geq 25°$, and subsequently refined by using higher angle data. These indicated a centered orthorhombic lattice. Data were collected for one independent octant, $+h,+k,+l$ by using the θ–2θ scan mode. The final scan speed for each reflection was determined from the net intensity gathered in an initial prescan and ranged from 2 to 7 deg min^{-1}. The ω-scan angle and aperture settings were determined as described in ref 6b. Crystal stability was monitored every 30 min throughout data collection by means of two check reflections. The systematic absences observed indicated either *Cmcm* or $Cmc2_1$ as the possible space groups. The former was adopted on the basis of successful refinement.

Data were corrected for the effects of Lorentz, polarization, decay, and absorption. An empirical, ψ-scan absorption correction was applied with transmission factors varying from 99.75% to 91.31%. Pertinent crystallographic and data collection parameters are collected in Table IX. The position of the cobalt atom was revealed from a Patterson map and all other non-hydrogen atoms from subsequent difference Fourier maps. In the final stages of refinement a weighting scheme of the form given in Table IX was introduced to downweight intense reflections. Final refinement using full-matrix least squares converged smoothly. No chemically significant peaks were present in the final difference map.

The details of the data collection and refinement for **4**, **6**, and **7** do not differ fundamentally from those described above for **1**. All relevant data are presented in Table IX. All calculations were carried out on a PDP 11-44 computer by use of the SDP Plus program package.[40]

Acknowledgment. We thank the National Science Foundation, the Robert A. Welch Foundation, the Research Corp. Trust (N.C.N.), and the Nuffield Foundation (N.C.N.) for financial support. We also thank Dr. W. Clegg for the use of graphics facilities used in drawing Figures 1–7, 10, and 11.

Registry No. **1**, 103257-59-6; **4**, 111464-90-5; **5**, 111349-06-5; **5a**, 111349-08-7; **6**, 111349-07-6; **7**, 111465-81-7; $Ar'PCl_2$, 79074-00-3; $(TMP)PCl_2$, 64945-24-0; Ar'P=PAr', 79073-99-7; $Ar'PH_2$, 83115-12-2; Ar'P(H)P(Cl)Ar', 110655-35-1; Ar'P(H)P(H)Ar', 83115-14-4; $K[Co(CO)_4]$, 14878-26-3; $K[Mo(CO)_3(\eta\text{-}(5H5)]$, 62866-01-7; $K[W(CO)_3(\eta\text{-}C_5H_5)]$, 62866-03-9; $Na_2[V(CO)_3(\eta\text{-}C_5H_5)]$, 68688-11-9; $[Co_2(CO)_6(\mu\text{-}PH)]$, 111349-09-8; $[V_2(CO),4\text{-}(\eta\text{-}C_5H_5)_2(\mu\text{-}PH)]$, 111349-10-1.

Supplementary Material Available: Tables of bond lengths, bond angles, and thermal parameters for **1**, **4**, **6**, and **7** and a table of calculated hydrogen positional parameters for **7** (19 pages); listings of observed and calculated structure factors for **1**, **4**, **6**, and **7** (42 pages). Ordering information is given on any current masthead page.

(40) *SDP Program Package*; B. A. Frenz and Associates, Inc.: College Station, TX.